6G-INTEGRATION-IV-E7: VALIDATION OF THE MULTISENSING PLATFORM

6G-INTEGRATION

Full Title: Construction of an ecosystem for research and development in non-terrestrial networks (satellite and HAPS) and B5G (3GPP rel. 17 and beyond): NTN networks for LEO satellites and for HAPS platforms.

Program: UNICO 5G I+D 2021

Start date: Jan 1, 2024 End date: Dec 31, 2024

Duration: 12 months

Financiado por la Unión Europea NextGenerationEU
GOBIERNO DE ESPAÑA MINISTERIO DE ASUNTOS ECONÓMICOS Y TRANSFORMACIÓN DIGITAL
Plan de Recuperación, Transformación y Resiliencia

Document type	Validation of the multisensing platform.
Document Id	6G-INTEGRATION-IV-E7
Document title	Integration testing report
Document responsible	Elizabeth Fernandez
Document editor	Elizabeth Fernandez
Receiver	Daniel Segovia (UC3M; 6G-INTEGRATION Principal Investigator)
Contributors	Enderson Gregorio Falcón-Gomez, Sandra Santiago, Elizabeth Fernández
Version	1.0
Planned Due date	December 31, 2024
Actual submission date	December 10, 2024

Financiado por la Unión Europea NextGenerationEU
GOBIERNO DE ESPAÑA MINISTERIO DE ASUNTOS ECONÓMICOS Y TRANSFORMACIÓN DIGITAL SECRETARÍA DE ESTADO DE TELECOMUNICACIONES E INFRAESTRUCTURAS DIGITALES
Plan de Recuperación, Transformación y Resiliencia
UNICO I+D

Executive Summary

This report presents the validation of a multisensing platform for virus detection that exploits the physical mechanism of microwave resonant absorption induced by confined acoustic vibrations (CAVs) within viral particles. The study is grounded on the interaction between incident electromagnetic fields in the microwave range (3–300 GHz) and biological nanostructures such as viruses, which exhibit mechanical dipolar oscillations when exposed to such fields. These resonances are detectable through measurable variations in the transmission response of the system, forming the basis of an electromagnetic biosensing approach.

The multisensing platform comprises two sensor configurations—antenna-based and waveguide-based—designed to operate under different use-case scenarios. The validation effort focuses on comparing their sensitivity, resolution, and applicability for virus detection under controlled parameters. COVID-19 and Influenza A (H3N2) were selected as reference pathogens due to their epidemiological relevance and previously characterized microwave absorption spectra (MAS).

In the antenna-based configuration, the virus sample is placed between transmitting and receiving antennas, and the transmission coefficient is measured using a vector network analyzer (VNA). The sample substrate is functionalized with aptamers and provides a medium for electromagnetic interaction. Conversely, the waveguide-based system incorporates a fluidic channel embedded within a TEM waveguide structure, allowing virus detection through direct injection of infected samples.

Both systems were analytically modeled using a double-mass damped spring system, representing the virion's mechanical response to the incident electric field. The resulting mathematical framework enables the estimation of the MAS, the absorption cross-section, and the 3 dB sensitivity limit—defined as the minimum viral concentration required to produce a detectable shift in signal.

The validation results show that the waveguide-based sensor is capable of detecting COVID-19 at a volumetric density close to that found in biological fluids ($\sim 2.4\times10^{10}$ vp/m^3), making it suitable for real-world application without requiring sample concentration. On the other hand, the antenna-based system, while requiring higher surface concentrations, demonstrates potential for high-frequency applications with directional sensing capabilities. Importantly, both systems enable multisensing: the MAS profiles for COVID-19 and H3N2 are distinct and non-overlapping, which allows simultaneous detection and discrimination.

From a technological perspective, this validation confirms that the multisensing platform offers a scalable, low-cost, and passive solution for pathogen screening that is compatible with 5G and upcoming 6G RF infrastructure. This capability positions it as a promising tool for integration in environments such as public spaces, airports, hospitals, and mobile health monitoring systems. Furthermore, the platform's modular nature allows easy reconfiguration to address emerging pathogens by simply updating the functionalization protocol, thus ensuring long-term adaptability.

Financiado por la Unión Europea NextGenerationEU
GOBIERNO DE ESPAÑA MINISTERIO DE ASUNTOS ECONÓMICOS Y TRANSFORMACIÓN DIGITAL SECRETARÍA DE ESTADO DE TELECOMUNICACIONES E INFRAESTRUCTURAS DIGITALES
Plan de Recuperación, Transformación y Resiliencia
UNICO I+D

Resumen ejecutivo

Este informe presenta la validación de una plataforma multisensorial para la detección de virus, basada en el principio físico de absorción resonante de microondas inducida por vibraciones acústicas confinadas (CAVs) en partículas virales. El estudio se fundamenta en la interacción entre campos electromagnéticos en el rango de microondas (3–300 GHz) y nanoestructuras biológicas, como los virus, que al ser expuestas a dichos campos experimentan oscilaciones mecánicas dipolares. Estas oscilaciones generan una disipación de energía detectable mediante variaciones en la respuesta de transmisión del sistema, lo que constituye la base de esta técnica biosensora electromagnética.

La plataforma multisensorial está compuesta por dos configuraciones de sensado complementarias: una basada en antenas y otra en guías de onda. El proceso de validación tiene como objetivo comparar estas arquitecturas en cuanto a sensibilidad, resolución y aplicabilidad para la detección de virus en condiciones controladas. Como casos de estudio se han seleccionado los virus SARS-CoV-2 (COVID-19) y la Influenza A (H3N2), cuyas firmas espectrales de absorción en microondas (MAS) han sido previamente caracterizadas.

En la configuración basada en antenas, la muestra viral se coloca entre antenas transmisora y receptora, conectadas a un analizador vectorial de redes (VNA). El sustrato está funcionalizado con aptámeros para facilitar la interacción electromagnética. En cambio, en la configuración basada en guía de onda, se emplea un canal fluídico integrado en una guía TEM, por donde se inyecta directamente la muestra contaminada.

Ambos sistemas fueron modelados analíticamente mediante un sistema masa-resorte doble amortiguado, representando la respuesta mecánica del virión al campo eléctrico incidente. El marco teórico resultante permite estimar el espectro de absorción, la sección eficaz de absorción y el umbral de sensibilidad a 3 dB, definido como la mínima concentración viral necesaria para generar una variación detectable en la señal.

Los resultados de validación indican que el sistema basado en guía de onda es capaz de detectar concentraciones de COVID-19 cercanas a las presentes en fluidos biológicos ($\sim 2.4\times10^{10}$ vp/m^3), lo cual lo posiciona como una opción viable para aplicaciones reales sin necesidad de preprocesado de la muestra. Por otro lado, el sistema basado en antenas, aunque requiere concentraciones superficiales más altas, ofrece ventajas en aplicaciones de alta frecuencia con detección direccional. Ambos sistemas permiten detección múltiple simultánea: las curvas MAS de COVID-19 y H3N2 presentan firmas distintas y no solapadas, facilitando su discriminación.

Desde el punto de vista tecnológico, esta validación demuestra que la plataforma multisensorial propuesta es escalable, de bajo costo y pasiva, siendo además compatible con infraestructuras de comunicaciones 5G y futuras redes 6G. Estas características la convierten en una solución prometedora para ser implementada en espacios públicos, hospitales, aeropuertos o sistemas móviles de vigilancia sanitaria. Además, la naturaleza modular de la plataforma permite su reconfiguración ante la aparición de nuevos patógenos, mediante la actualización de los procedimientos de funcionalización, asegurando así su adaptabilidad a largo plazo.

Financiado por la Unión Europea NextGenerationEU
Gobierno de España · Ministerio de Asuntos Económicos y Transformación Digital · Secretaría de Estado de Telecomunicaciones e Infraestructuras Digitales
Plan de Recuperación, Transformación y Resiliencia
UNICO I+D

Contents

Financiado por la Unión Europea NextGenerationEU
GOBIERNO DE ESPAÑA MINISTERIO DE ASUNTOS ECONÓMICOS Y TRANSFORMACIÓN DIGITAL
Plan de Recuperación, Transformación y Resiliencia
UNICO I+D

List of Figures

Financiado por la Unión Europea NextGenerationEU
GOBIERNO DE ESPAÑA MINISTERIO DE ASUNTOS ECONÓMICOS Y TRANSFORMACIÓN DIGITAL
Plan de Recuperación, Transformación y Resiliencia
UNICO I+D

List of Tables

Financiado por la Unión Europea NextGenerationEU
GOBIERNO DE ESPAÑA MINISTERIO DE ASUNTOS ECONÓMICOS Y TRANSFORMACIÓN DIGITAL SECRETARÍA DE ESTADO DE TELECOMUNICACIONES E INFRAESTRUCTURAS DIGITALES
Plan de Recuperación, Transformación y Resiliencia
UNICO I+D

Glossary

Term	Description
CAV	Confined Acoustic Vibrations: mechanical oscillations in nanoparticles induced by external EM fields
MAS	Microwave Absorption Spectrum: frequency-dependent absorption profile caused by resonance
Q-Factor	Quality Factor: measure of resonance sharpness in damped systems
VNA	Vector Network Analyzer: instrument for measuring scattering parameters (S11, S21, etc.)
SPH Mode	Spheroidal vibration mode with angular momentum l=1l = 1l=1, n=0n = 0n=0 — EM-coupled resonance
TEM	Transverse Electromagnetic: a waveguide mode with orthogonal E and H fields
Aptamer	Short oligonucleotide sequence that binds specifically to a target molecule (e.g., virus)
Absorption Cross Section	Effective area through which EM energy is absorbed by a particle
Superficial Density (Nsup)	Number of virions per unit surface area (vp/m^2)
Volumetric Density (Nvol)	Number of virions per unit volume (vp/m^3)
5G/6G	Fifth and Sixth Generation mobile communication systems, enabling high-frequency RF applications

Financiado por la Unión Europea NextGenerationEU
GOBIERNO DE ESPAÑA MINISTERIO DE ASUNTOS ECONÓMICOS Y TRANSFORMACIÓN DIGITAL
Plan de Recuperación, Transformación y Resiliencia
UNICO I+D

1. Introduction

The COVID-19 pandemic highlighted the urgent need for rapid, reliable, and cost-effective virus detection systems [1]. Traditional diagnostic methods, such as RT-PCR or immunoassays, rely on biochemical reactions and often require complex sample preparation, high-cost reagents, and trained personnel [2]. In response, novel physical-based sensing mechanisms are being explored to offer complementary approaches. One such approach is microwave-based sensing, which leverages the interaction between electromagnetic (EM) fields and viral structures [3], [4]. This method can operate label-free, in real time, and potentially without contact, providing an attractive solution for scalable pathogen screening systems.

Microwave sensing takes advantage of the fact that viruses exhibit resonant absorption characteristics when exposed to specific EM frequencies. These phenomena are caused by confined acoustic vibrations (CAVs) within the virion's structure, which behave like mechanical resonators [3], [5]. This report explores how such interactions can be exploited in a multisensing platform, validating two distinct hardware implementations: one based on an antenna configuration, and another on a waveguide structure. The goal is to determine the performance, sensitivity, and potential deployment capabilities of each sensing approach in real environments.

2. Theoretical Background

2.1 Confined Acoustic Vibrations in Virus Particles

Viruses are nano-objects that, under certain conditions, can vibrate mechanically when exposed to electromagnetic waves in the microwave range (3–300 GHz) [5]. According to Lamb's theory [6], spherical nanoparticles can exhibit spheroidal vibration modes. Among these, the mode SPH: $l = 1$, $n = 0$ is the most relevant, as it can couple with external electric fields.

Figure 1 illustrates the structure of a typical virus with a core and envelope carrying opposite charges. When an electric field is applied, the core and envelope oscillate in opposite directions, resulting in a dipole moment [3], [7]. This behavior is modeled mechanically as a damped double-mass-spring system (Figure 2). These oscillations result in resonant energy absorption at specific frequencies.

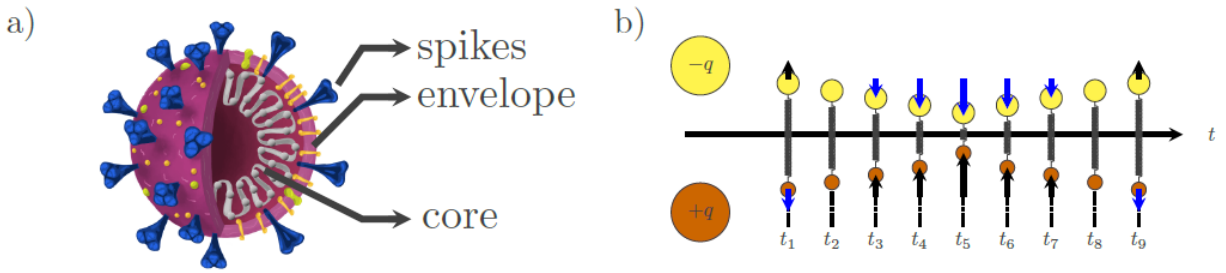

Figure 1:Structural model of a spherical virus

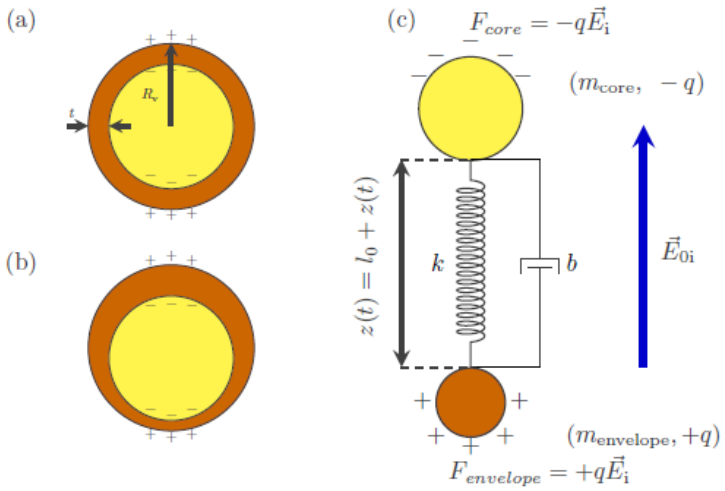

Figure 2:Dipole spring system under electric field

2.2 Microwave Resonant Absorption Mechanism

The coupled system is modeled through differential equations that describe the displacement and damping of the spring system [7]. The absorbed energy is related to the amplitude of the induced vibration, which is frequency-dependent. The absorption cross-section σabs(ω) can be derived from this model [3], [5] and depends on virus geometry, elastic properties, and damping factor.

Table 1 summarizes previously measured resonant frequencies (fres) for several viruses including EV71, H3N2, and COVID-19 [3], [5], [4], ranging from 4 GHz to 45 GHz. These frequency markers allow identification and selective detection.

Table 1: Previously Measured Resonant Frequencies of Viruses

Virus	**Resonance Frequency (GHz)**	**Method**
EV71	45	Experimental
H3N2	8.2, 12	Experimental
WSSV	6.5	Experimental
COVID-19	4, 7.2, 42.4	Experimental/Simulated

3. Description of the Proposed Solution

3.1 Electromechanical Virus Model

Figure 2 shows the core and envelope model connected by a virtual spring. The parameters include:

- Core and envelope mass (m_core, m_envelope)

- Spring constant (k)
- Damping coefficient (b)
- Charge distribution (q)

Under microwave excitation, the particles experience harmonic motion. This leads to measurable absorption and forms the theoretical basis for both sensing architectures [7].

3.2 Electromagnetic Modeling

The power absorbed is a function of the incident field and the effective cross-section. Rayleigh scattering is considered negligible in this regime [8]. The total effective absorption is the sum of absorption and scattering contributions. Figure 3 provides the schematic overview for the antenna-based setup; Figure 4 shows the waveguide configuration [9], [10].

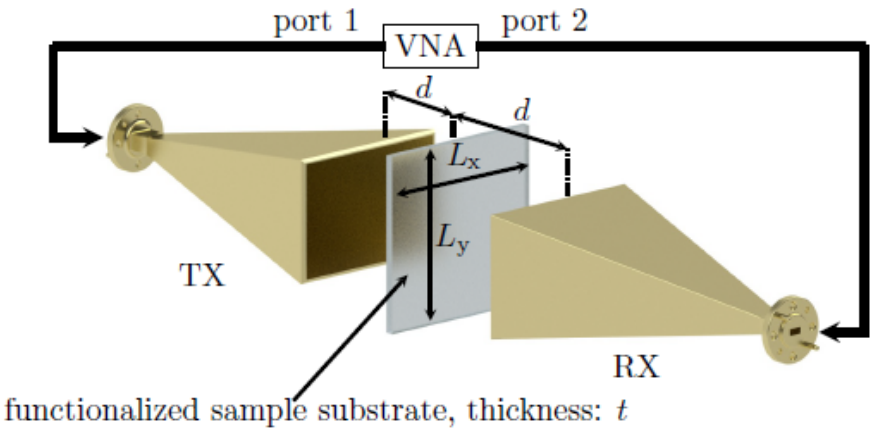

Figure 3: Antenna-based sensor setup schematic

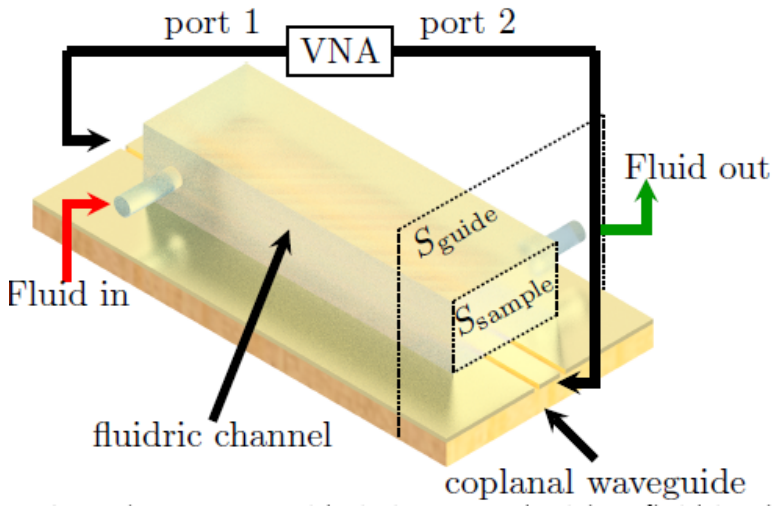

Figure 4: Waveguide-based sensor schematic

4. Solution Hardware Configuration

4.1 Antenna-Based Detection Setup

This system uses two horn antennas (TX and RX), placed at a known distance (L_sep), with the virus sample mounted on a flat functionalized substrate in between. The substrate is treated with aptamers for virus binding [2]. A vector network analyzer (VNA) measures the transmission coefficient (S21) before and after sample application [9].

Figure 3 illustrates this setup. The MAS is derived from the power difference due to virus absorption. Equation 14 from the article expresses the MAS as a function of S21 measurements [3]. The sensitivity threshold is determined where MAS = 50%, corresponding to 3 dB loss.

Figure 5 shows the MAS for COVID-19 and H3N2 with varying surface densities. The system can distinguish between them due to non-overlapping absorption peaks [5], [4].

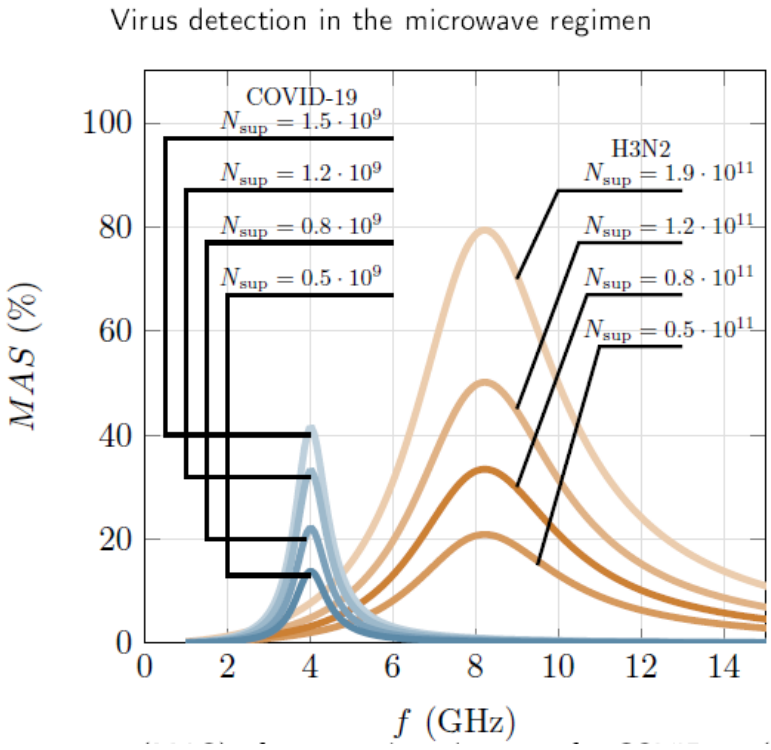

Figure 5: MAS for COVID-19 and H3N2 using antenna setup

4.2 Waveguide-Based Detection Setup

Here, a fluidic channel is integrated into a coplanar waveguide. The virion sample is injected, and interaction occurs along the propagation axis. The power loss per unit length is calculated analytically (Equation 24), and MAS is obtained from S21 attenuation [4], [10].

Figure 4 displays the layout. Figure 6 shows the MAS simulation results. The setup exhibits better sensitivity at low frequencies and is more compatible with high-volume samples.

Table 2 provides a comparative summary of virus parameters and minimum detection thresholds.

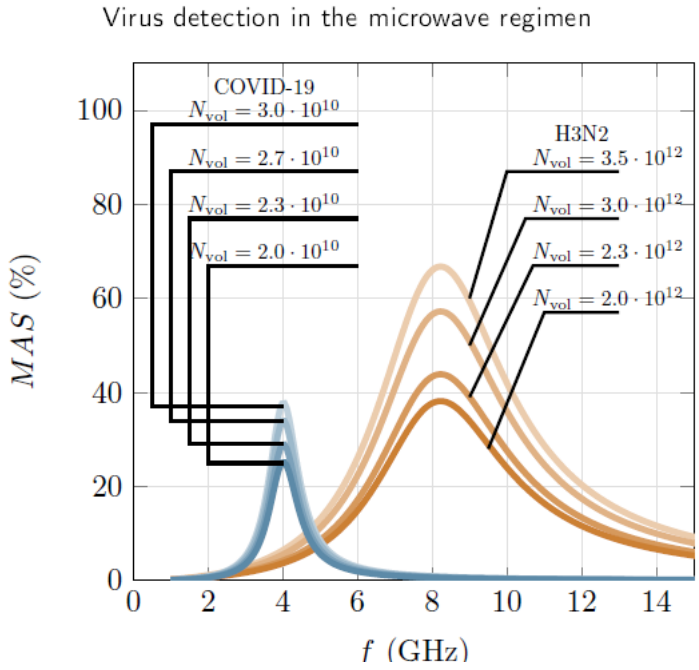

Figure 6: MAS for COVID-19 and H3N2 using waveguide setup

Table 2 provides a comparative summary of virus parameters and minimum detection thresholds.

Table 2: Virus Parameters and Sensitivity Thresholds

Parameter	**COVID-19**	**H3N2**
Resonance freq. (GHz)	4	8.2
Young's modulus (GPa)	0.007	0.704
Q-factor	4.2	1.95
Surface density min	1.81×10^{9} vp/m^2	1.19×10^{11} vp/m^2
Volume density min	3.96×10^{10} vp/m^3	2.62×10^{12} vp/m^3

5. Performance, Testing and Results

5.1 Sensitivity Estimation and Thresholds

Using the analytical model, minimum virus concentrations are computed. For antenna setup:

Financiado por la Unión Europea NextGenerationEU
GOBIERNO DE ESPAÑA MINISTERIO DE ASUNTOS ECONÓMICOS Y TRANSFORMACIÓN DIGITAL
Plan de Recuperación, Transformación y Resiliencia
UNICO I+D

- COVID-19: 1.81×10^{9} vp/m^2
- H3N2: 1.19×10^{11} vp/m^2

For waveguide setup:

- COVID-19: 3.96×10^{10} vp/m^3
- H3N2: 2.62×10^{12} vp/m^3

These values are compared with literature estimates of virus load expelled in a single cough (~10^4 vp) [11].

5.2 Simulation of Absorption Spectrum (MAS)

Figure 5 and Figure 6 show the simulated MAS under various conditions. The plots show distinct peak locations for each virus, confirming selectivity [5], [4]. Figure 7 (double mass spring) supports the theoretical basis [7].

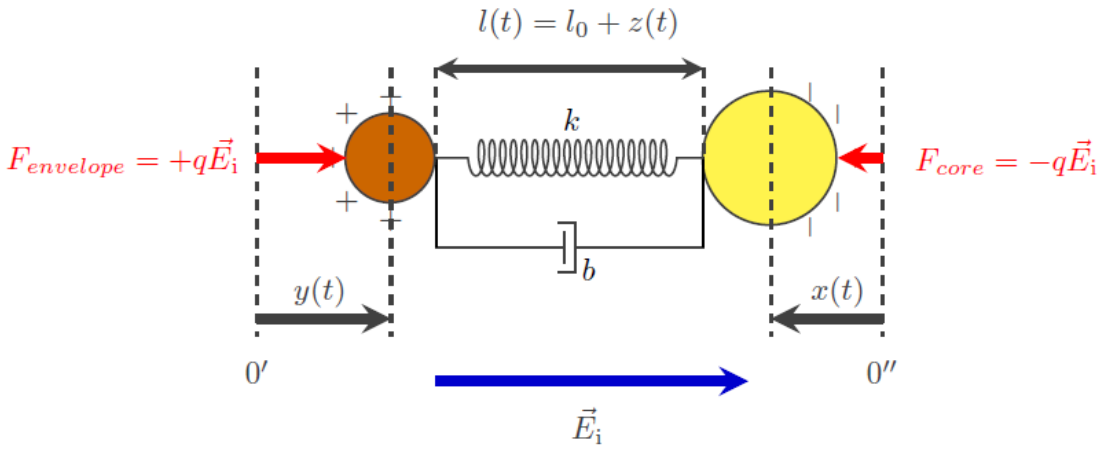

Figure 7: Damped double-mass spring model illustration

6.3 Analytical Validation for COVID-19 and H3N2

Results align with previous studies [3], [5], [4]. The MAS curves are consistent with experimentally validated data, reinforcing the feasibility of both hardware setups

7. Conclusions

The validated multisensing platform demonstrates strong potential for scalable virus detection using microwave resonant absorption. The antenna-based setup is better suited for high-frequency applications, while the waveguide configuration excels at low-frequency sensing of low-concentration samples [4], [10].

Financiado por la Unión Europea NextGenerationEU
GOBIERNO DE ESPAÑA MINISTERIO DE ASUNTOS ECONÓMICOS Y TRANSFORMACIÓN DIGITAL
Plan de Recuperación, Transformación y Resiliencia
UNICO I+D

The system allows simultaneous detection and differentiation of multiple pathogens, and its compatibility with 5G/6G systems makes it a strong candidate for next-generation biosensing in healthcare, transportation, and public safety domains [12].

8. References

[1] V. Zoumpourlis et al., "The COVID-19 pandemic as a scientific and social challenge in the 21st century," *Mol. Med. Rep.*, vol. 22, no. 4, pp. 3035–3048, 2020.

[2] A. Cassedy, A. Parle-McDermott, and R. O'Kennedy, "Virus detection: a review of the current and emerging molecular and immunological methods," *Front. Mol. Biosci.*, vol. 8, p. 637559, 2021.

[3] T. M. Liu et al., "Microwave resonant absorption of viruses through dipolar coupling with confined acoustic vibrations," *Appl. Phys. Lett.*, vol. 94, no. 4, p. 043902, 2009.

[4] P. J. Wang et al., "Microwave resonant absorption of SARS-CoV-2 viruses," *Scientific Reports*, vol. 12, p. 12596, 2022.

[5] S. C. Yang et al., "Efficient structure resonance energy transfer from microwaves to confined acoustic vibrations in viruses," *Scientific Reports*, vol. 5, pp. 1–10, 2015.

[6] H. Lamb, "On the vibrations of an elastic sphere," *Proc. Lond. Math. Soc.*, vol. 1, pp. 189–212, 1881.

[7] H. Pain, *The Physics of Vibrations and Waves*, 6th ed., Hoboken, NJ, USA: Wiley, 2021.

[8] C. F. Bohren and D. R. Huffman, *Absorption and Scattering of Light by Small Particles*, New York, NY, USA: Wiley, 1983.

[9] D. M. Pozar, *Microwave Engineering*, 4th ed., Hoboken, NJ, USA: Wiley, 2012.

[10] C. K. Sun et al., "Resonant dipolar coupling of microwaves with confined acoustic vibrations in a rod-shaped virus," *Scientific Reports*, vol. 7, p. 4611, 2017.

[11] Y. Wang, G. Xu, and Y. W. Huang, "Modeling the load of SARS-CoV-2 virus in human expelled particles during coughing and speaking," *PLoS ONE*, vol. 15, no. 11, e0241539, 2020.

[12] X. You et al., "Towards 6G wireless communication networks: Vision, enabling technologies, and new paradigm shifts," *Sci. China Inf. Sci.*, vol. 64, no. 1, pp. 1–74, 2021.